



HHS Public Access

Author manuscript

Nature. Author manuscript; available in PMC 2011 January 01.

Published in final edited form as:

Nature. 2010 July 15; 466(7304): 373–377. doi:10.1038/nature09179.

Blindsight depends on the lateral geniculate nucleus

Michael C. Schmid¹, Sylwia W. Mrowka¹, Janita Turchi¹, Richard C. Saunders¹, Melanie Wilke¹, Andrew J. Peters¹, Frank Q. Ye², and David A. Leopold^{1,2}

¹Laboratory of Neuropsychology, NIMH, NINDS, NEI, 49 Convent Drive, Bethesda, MD, 20892, USA.

²Neurophysiology Imaging Facility, NIMH, NINDS, NEI, 49 Convent Drive, Bethesda, MD, 20892, USA.

Abstract

Injury to the primary visual cortex (V1) leads to the loss of visual experience. Nonetheless, careful testing shows that certain visually guided behaviors can persist even in the absence of visual awareness^{1–5}. The neural circuits supporting this phenomenon, often termed blindsight, remain uncertain⁵. Here we demonstrate a causal role of the thalamic lateral geniculate nucleus (LGN) in V1-independent processing of visual information. By comparing fMRI and behavioral measures with and without temporary LGN inactivation, we assessed the contribution of the LGN to visual functions of macaque monkeys with chronic V1 lesions. Prior to LGN inactivation, high contrast stimuli presented to the lesion-affected visual field (scotoma) produced significant V1 independent fMRI activation in extrastriate cortical areas V2, V3, V4, V5/MT, FST, and LIP, and were correctly located by the animals in a detection task. However, following reversible inactivation of the LGN in the V1-lesioned hemisphere both fMRI responses and behavioral detection were abolished. Taken together, these results demonstrate a critical functional contribution of the direct LGN projections to extrastriate cortex in blindsight, and suggest a viable pathway mediating fast detection during normal vision.

Two adult macaque monkeys with chronic V1 aspiration lesions (methods summary) were acclimated to the functional magnetic resonance imaging (fMRI) testing environment. During the experiments the animals sat upright in a custom-made chair placed in a vertical 4.7 Tesla MR scanner and fixated a small point in the center of the screen while the eye position was recorded and visual stimuli were presented (supplementary methods). The boundaries of retinotopically organized visual areas were established using standard functional mapping methods (supplementary figures 1 and 2)⁶. The center of the lesion was located at the representation of the horizontal meridian and extended several millimeters

Users may view, print, copy, download and text and data- mine the content in such documents, for the purposes of academic research, subject always to the full Conditions of use: http://www.nature.com/authors/editorial_policies/license.html#terms

Correspondence should be addressed to MCS (schmidmicha@gmail.com).

Author contributions: MCS took the primary lead for all aspects of this work and wrote the paper; SM helped with performing experiments and analysis; JT helped performing the experiments and developed the inactivation method; RS performed the lesions; MW developed the inactivation method; AJP helped with performing experiments and analysis; FQY developed pre-processing software and optimized MR sequences, DAL provided resources, acted in a supervisory role on all aspects of this work and wrote the paper.

both dorsally and ventrally into V1 (black area in figure 1a, area between red bars in figure 1b, black area in supplementary figure 2), corresponding to a visual eccentricity of ~ 2 to ~ 7 degrees of visual angle. Previous work has shown that this type of lesion in V1 does not alter the retinotopic organization assessed with fMRI in several extrastriate areas⁷.

To assess whether extrastriate cortex could be activated in the absence of V1 input, we presented a small (2° diameter), rotating checkerboard pattern, known to effectively drive responses in early visual cortex, to the visual field region affected by the lesion (scotoma, figure 1c, upper panel), and in independent experimental runs to the corresponding region in the healthy hemisphere as a control (figure 1c, lower panel). As expected, the stimulus shown to the unaffected hemifield elicited strong, circumscribed, contralateral responses in V1, neighboring extrastriate areas V2/V3, V4, V5/MT and FST (figure 2 a,d), and in parietal area LIP (supplementary figure 3 a,c). When the stimulus was presented inside the scotoma region, there was no V1 response (since the cortex was removed); nonetheless, there were stimulus-driven responses in extrastriate areas V2/V3, V4, V5/MT, FST and LIP (figure 2 b,e; supplementary figure 3 b,d), indicating that stimulus information reached these areas in the absence of V1 input. Moreover, comparing the activation patterns of the lesioned and control hemisphere revealed that the responses within each area were localized to their normal retinotopic positions. However, one prominent difference between the lesioned and the control conditions was the emergence of a dorsoventral asymmetry in areas V2 and V3, with only dorsal, but not ventral portions of these areas exhibiting V1-independent responses. This effect, which has been previously observed in human blindsight⁸, cannot be attributed to the position of either the lesion or the stimulus, since the retinotopically-matched stimulus in the opposite visual field evoked roughly equivalent responses in both dorsal and ventral parts.

On the behavioral level, both monkeys retained the ability to detect and make a saccadic eye movement to small (0.2° diameter), high, but not low, contrast visual targets presented inside the scotoma albeit with a diminished performance. Target contrasts were adjusted based on performance in the control hemifield, such that there was reliable detection even at the lowest contrast level (7%) (figure 2c,f, and supplementary methods). When low contrast stimuli were presented inside the scotoma, both monkeys consistently maintained central fixation, indicating they were probably unaware of any stimulus being presented³. By comparison, when high contrast (100%) stimuli were shown, the monkeys were able to detect roughly half the presentations, consistent with previous reports of blindsight in humans and monkeys 1–4,9. Finally, a direct comparison between detection performance and fMRI responses to the same set of stimuli (2° diameter) presented in the scotoma at varying luminance contrast levels confirmed the tight relationship between both measures of blindsight (supplementary figure 4).

Several controls ruled out the possibility of scattered light contributing to the observed effects^{10,11}. First, behavioral responses were spatially accurate, since performance was calculated by only considering saccades that were within 1° from the target. Second, when the same, high-contrast stimuli were presented monocularly in the monkey's blindspot (area covered by the optic disc in the retina), performance fell to zero (supplementary figure 5). Third, no systematic fMRI modulation was measured in intact V1 of either monkey adjacent

to the lesion (figure 2b, e). Fourth, strong extrastriate activation was found in a third monkey, in which a much larger lesion was made, encompassing all of opercular V1 and a portion of adjacent V2 (supplementary figure 6). Taken together, these experiments rule out non-specific effects of scattering light^{10,11} as being responsible for the observed behavioral and fMRI responses to stimuli in the scotoma, and demonstrate a viable visual pathway that can operate in the absence of V1, in accordance with previous studies in human patients and lesion studies in monkeys^{1–5,7,8,12,13}.

We next asked, what are the components of the pathway that provide V1-bypassing input to the extrastriate cortex and that support visual performance? Previous work has demonstrated the existence of direct anatomical projections from the LGN, the main thalamic relay between the retina and the primary visual cortex, to several extrastriate visual areas^{14,15}. We therefore hypothesized that residual activity in extrastriate cortex and corresponding behavioral performance is the result of sensory signals transmitted directly from the LGN. We examined this possibility by temporarily disrupting neural activity within the LGN of V1-lesioned monkeys by locally injecting the GABA-A agonist THIP¹⁶ (methods summary), and measuring the effects on both cortical fMRI responses and behavioral performance. Specifically, the posterior part of the LGN, which represents the parafoveal visual hemifield and covers the scotoma-affected region (methods summary), was reversibly inactivated on multiple occasions via chronically implanted MR-compatible guide tubes. The MR contrast agent gadolinium (Gd) was co-injected along with THIP, allowing for the visualization of the spread of the injection in the tissue. In both monkeys (figure 3 a,d), the 2 μ l injection diffused to an effective diameter of approximately 3 mm in the caudal LGN, as visualized by the Gd (figure 3 a, d, ~ AP+7 in stereotactic coordinates).

Following inactivation of the LGN virtually all extrastriate responses in the V1-lesioned hemispheres disappeared, (figure 3 b,e), indicating that the residual activation to stimuli presented in the scotoma had reached extrastriate cortex via direct projections from the LGN. Moreover, inactivation of the LGN abolished the animals' residual capacity to detect high contrast stimuli presented to the scotoma region of the visual field (red line, figure 3 c,f), demonstrating that the LGN is the critical thalamic link supporting behavioral performance in blindsight. Detection of visual control stimuli in the opposite hemifield (outside the scotoma) remained unaffected.

To obtain a more quantitative assessment of the amount of information transmitted via the LGN directly, we compared the strength of fMRI responses under normal visual stimulation conditions to those obtained inside the scotoma, with and without additional LGN inactivation, across all experimental sessions (figure 4). On average, across monkeys and extrastriate areas, fMRI activation levels to scotoma stimulation with the LGN intact were ~20% compared to normal conditions. This finding is in good qualitative agreement with previously reported fMRI activation patterns of human and monkey blindsight subjects^{7,8,12} and with single unit recordings in area V5/MT of macaque monkeys with chronic V1 lesions¹³. Inactivating the LGN in addition reduced activation levels to less than 5% compared to normal.

Aside from demonstrating the role of the LGN in supporting blindsight, these data reveal several interesting features of V1-independent vision. For example, the asymmetry of visual responses in areas V2/V3 to stimuli in the scotoma, which has been previously observed in blindsight patient GY8, may reflect the differential contributions of parallel visual streams to upper and lower field vision. Namely, a larger proportion of neurons in both in the retina and LGN respond to lower than to upper visual field stimulation¹⁷. Psychophysical evidence suggests that this bias is primarily related to the magnocellular system¹⁸, which at the level of the retina is also the system that is less affected by retrograde degeneration following V1 injury¹⁹. Thus, one possibility for the observed asymmetry following striate cortex lesions is that the normal visual field asymmetry of the magnocellular system is unmasked by post-lesional neurodegeneration.

The near-complete drop in both extrastriate activation and behavioral performance not only implicate the LGN as being a critical hub for blindsight, but also argues against pathways that do not involve the LGN. Blindsight functions have been observed for decades in a number of different species and have traditionally been attributed to a second visual pathway where retinal information is relayed via the superior colliculus and another, secondary thalamic nucleus, the pulvinar, to the extrastriate cortex²⁰. While the role of the superior colliculus in mediating blindsight functions and V1-independent responses in area V5/MT of humans and monkeys has been demonstrated^{21,22}, there is presently no direct evidence for a role of the pulvinar. On the contrary, the pulvinar may have minimal contribution for the following reasons: (i) its anatomical basis as a first order visual relay are in question²³, (ii) its neural responses appear to be driven more by cortical than by collicular inputs²⁴, (iii) there is no residual vision following LGN lesions²⁵, and (iv) neural activity in area V5/MT is eliminated during LGN inactivation²⁶.

Conversely, contribution of the LGN to blindsight has sometimes been left as an open possibility^{5,22}, though post-lesional degeneration of the parvo- and magnocellular layers within the LGN has raised question as to how a viable pathway would survive¹⁹. Our demonstration of a functional route through the LGN may therefore point to the involvement of the koniocellular system, whose neurons reside primarily in the intercalated layers, which have been shown to survive following V1 lesions²⁷. Interestingly, it is also these same koniocellular-rich layers that receive input from the superior colliculus^{23,28} and that project directly to area V5/MT and possibly also to other extrastriate cortical areas^{14,15}, which may explain the previously described effects of superior colliculus ablation on V1-independent visual processing^{21,22}. Finally, recent observations using diffusion tensor MR imaging in a human blindsight patient many years after a V1 lesion demonstrate significant projections between the LGN and area V5/MT²⁹, although the directionality of the projection could not be established with that method.

Taken together, our data demonstrate a causal role of the LGN for V1-independent visual functions. We hypothesize that this residual function is mediated by neurons in the intercalated layers of the LGN, whose direct projections to the extrastriate cortex may not only support residual vision following V1 lesions, but which may also serve as a shortcut to high-level cortex during normal vision. This shortcut may serve to explain the very short

latency neural responses observed in some extrastriate visual areas³⁰, and may facilitate some forms of rapid behavioral responses to visual stimuli.

Methods summary

The main experiments were carried out in two healthy adult monkeys (*Macaca mulatta*), one male (8 kg weight) and one female (5 kg weight). Additional control experiments were conducted in a third healthy adult female monkey (5 kg weight). All procedures followed the ILAR (Institute of Laboratory Animal Resources, National Research Council of the National Academy of Sciences) guidelines and were approved by the NIMH Animal Care and Use Committee of the US National Institutes of Health (National Institute of Mental Health). To immobilize the head during experiments and record eye movements during behavioral testing, headposts and eye coils were implanted following standard procedures described elsewhere¹⁶. Area V1 lesions were performed by coagulating pial vessels over the intended lesion area on the V1 operculum and by aspirating gray matter within this area. In both monkeys the lesions were located ~2–7° visual eccentricities away from the fovea (monkeys had no problems maintaining fixation), covering between one third and one half of opercular V1. A lesion in a third monkey, completely covering opercular V1 and also large parts of adjacent V2 (supplementary figure 6), was used to evaluate the possibility of scattered light effects on intact gray matter tissue in the first two monkeys with smaller lesions. To reach the LGN for inactivation, MR-compatible fused-silica guide tubes (Plastics One, Roanoke, VA) were chronically implanted in monkeys 1 and 2, using a frameless stereotaxy procedure (Brainsight, Rogue Research, Montreal, Canada). For the experiments, the GABA-A agonist THIP (Tocris; Concentration: 6.67µg/µl, dissolved in sterile saline, pH 7.4; Volume: 2µl; Rate: 0.5 – 1µl/min) was injected for LGN inactivation together with the MR contrast agent Gadolinium (Berlex Imaging, 5mM) to visualize the site and extent of the injection in an MR image.

Supplementary Material

Refer to Web version on PubMed Central for supplementary material.

Acknowledgements

We would like to thank Drs. Alex Maier and David McMahon for comments on the manuscript, and Drs. Stelios Smirnakis, Rebecca Berman, Bob Wurtz, Barry Richmond, Sebastian Guderian & Makoto Fukushima for helpful discussions, Charles Zhu and Dr. Hellmut Merkle for MR coil construction, Katy Smith, Neal Phipps, James Yu, George Dold, David Ide and Tom Talbot for technical assistance, Dr. David Sheinberg for the development of visual stimulation software & members of the Brian Wandell lab for developing and sharing mrvista software. This work was supported by the Intramural Research Program of NIMH, NINDS, and NEI.

References

1. Sanders MD, Warrington EK, Marshall J. "Blindsight": Vision in a field defect. *Lancet*. 1974
2. Weiskrantz L, Warrington EK, Sanders MD. Visual capacity in the hemianopic field following a restricted occipital ablation. *Brain*. 1974
3. Cowey A, Stoerig P. Blindsight in monkeys. *Nature*. 1995; 373:247–249. [PubMed: 7816139]
4. Keating EG. Residual spatial vision in the monkey after removal of striate and preoccipital cortex. *Brain Res*. 1980; 187:271–290. [PubMed: 6768421]

5. Cowey A. The blindsight saga. *Exp Brain Res.* 2009;1–22. doi:10.1007/s00221-009-1914-2.
6. Brewer AA, Press WA, Logothetis NK, Wandell BA. Visual Areas in Macaque Cortex Measured Using Functional Magnetic Resonance Imaging. *J. Neurosci.* 2002; 22:10416–10426. [PubMed: 12451141]
7. Schmid MC, Panagiotaropoulos T, Augath MA, Logothetis NK, Smirnakis SM. Visually driven activation in macaque areas V2 and V3 without input from the primary visual cortex. *PLoS ONE.* 2009; 4:e5527. doi:10.1371/journal.pone.0005527. [PubMed: 19436733]
8. Baseler HA, Morland AB, Wandell BA. Topographic Organization of Human Visual Areas in the Absence of Input from Primary Cortex. *J. Neurosci.* 1999; 19:2619–2627. [PubMed: 10087075]
9. Cowey A, Stoerig P. Visual detection in monkeys with blindsight. *Neuropsychologia.* 1997
10. Collins CE, Lyon DC, Kaas JH. Responses of neurons in the middle temporal visual area after long-standing lesions of the primary visual cortex in adult new world monkeys. *J Neurosci.* 2003; 23:2251–2264. [PubMed: 12657684]
11. Campion J, Latto R, Smith YM. *Behav Brain Sci.* 1983; Vol. 6:423–447.
12. Goebel R, Muckli L, Zanella FE, Singer W, Stoerig P. Sustained extrastriate cortical activation without visual awareness revealed by fMRI studies of hemianopic patients. *Vision Res.* 2001; 41:1459–1474. [PubMed: 11322986]
13. Rodman HR, Gross CG, Albright TD. Afferent basis of visual response properties in area MT of the macaque. I. Effects of striate cortex removal. *J Neurosci.* 1989; 9:2033–2050. [PubMed: 2723765]
14. Sincich LC, Park KF, Wohlgenuth MJ, Horton JC. Bypassing V1: a direct geniculate input to area MT. *Nat Neurosci.* 2004; 7:1123–1128. [PubMed: 15378066]
15. Fries W. The projection from the lateral geniculate nucleus to the prestriate cortex of the macaque monkey. *Proc R Soc Lond B Biol Sci.* 1981; 213:73–86. [PubMed: 6117869]
16. Cope DW, Hughes SW, Crunelli V. GABAA receptor-mediated tonic inhibition in thalamic neurons. *J Neurosci.* 2005; 25:11553–11563. [PubMed: 16354913]
17. Curcio CA, Allen KA. Topography of ganglion cells in human retina. *J Comp Neurol.* 1990; 300:5–25. doi:10.1002/cne.903000103. [PubMed: 2229487]
18. McAnany JJ, Levine MW. Magnocellular and parvocellular visual pathway contributions to visual field anisotropies. *Vision Res.* 2007; 47:2327–2336. [PubMed: 17662333]
19. Cowey A, Stoerig P, Perry VH. Transneuronal retrograde degeneration of retinal ganglion cells after damage to striate cortex in macaque monkeys: selective loss of P beta cells. *Neuroscience.* 1989; 29:65–80. [PubMed: 2710349]
20. Diamond IT, Hall WC. Evolution of neocortex. *Science.* 1969; 164:251–262. [PubMed: 4887561]
21. Mohler CW, Wurtz RH. Role of striate cortex and superior colliculus in visual guidance of saccadic eye movements in monkeys. *J Neurophysiol.* 1977; 40:74–94. [PubMed: 401874]
22. Rodman HR, Gross CG, Albright TD. Afferent basis of visual response properties in area MT of the macaque. II. Effects of superior colliculus removal. *J Neurosci.* 1990; 10:1154–1164. [PubMed: 2329373]
23. Stepniewska I, Qi HX, Kaas JH. Do superior colliculus projection zones in the inferior pulvinar project to MT in primates? *Eur J Neurosci.* 1999; 11:469–480. [PubMed: 10051748]
24. Bender DB. Visual activation of neurons in the primate pulvinar depends on cortex but not colliculus. *Brain Res.* 1983; 279:258–261. [PubMed: 6640346]
25. Schiller PH, Sandell JH, Maunsell JH. The effect of lateral geniculate lesions on the detection of visual stimuli. *Investigative Ophthalmology and Visual Science.* 1985; 26:S-195.
26. Maunsell JH, Nealey TA, DePriest DD. Magnocellular and parvocellular contributions to responses in the middle temporal visual area (MT) of the macaque monkey. *J Neurosci.* 1990; 10:3323–3334. [PubMed: 2213142]
27. Cowey A, Stoerig P. Projection patterns of surviving neurons in the dorsal lateral geniculate nucleus following discrete lesions of striate cortex: implications for residual vision. *Exp Brain Res.* 1989; 75:631–638. [PubMed: 2744120]
28. Harting JK, Huerta MF, Hashikawa T, van Lieshout DP. Projection of the mammalian superior colliculus upon the dorsal lateral geniculate nucleus: organization of tectogeniculate pathways in

- nineteen species. *J Comp Neurol.* 1991; 304:275–306. doi:10.1002/cne.903040210. [PubMed: 1707899]
29. Bridge H, Thomas O, Jbabdi S, Cowey A. Changes in connectivity after visual cortical brain damage underlie altered visual function. *Brain.* 2008; 131:1433–1444. doi:10.1093/brain/awn063. [PubMed: 18469021]
30. Schmolesky MT, et al. Signal timing across the macaque visual system. *J Neurophysiol.* 1998; 79:3272–3278. [PubMed: 9636126]

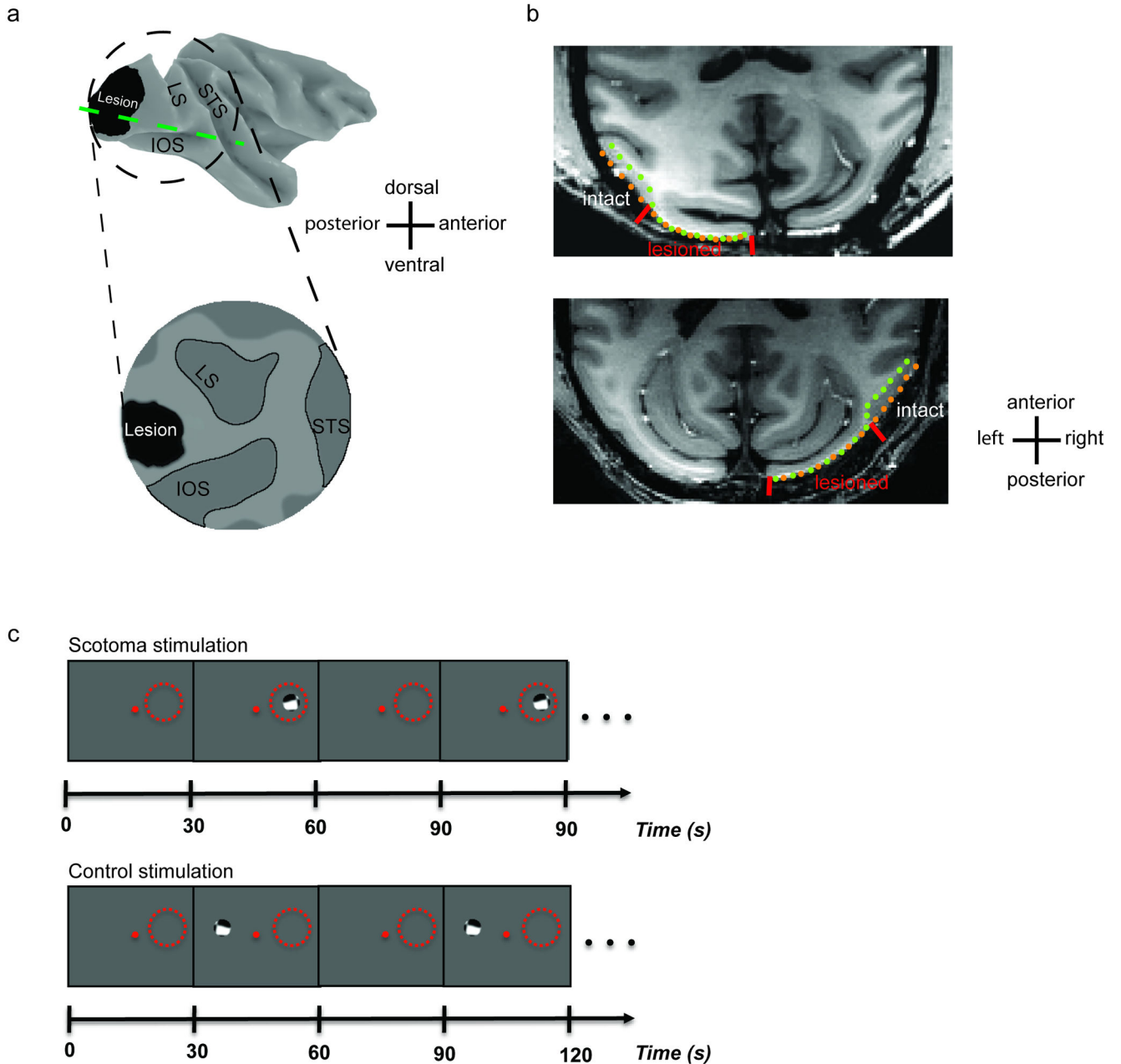


Figure 1.

Experimental setup. **a**. The upper part shows a side view on the right hemisphere of an inflated macaque brain. An area of $\sim 400 \text{ mm}^2$ of gray matter in the opercular part of primary visual cortex (V1) representing the visual field between $\sim 2^\circ$ and 7° has been surgically aspirated and is shown in black. Extrastriate areas, the subject of analysis in this study, are hidden in the sulci surrounding V1, including the lunate (LS), inferior occipital (IOS), and superior temporal (STS) sulci. To facilitate the visual examination of extrastriate cortex, the occipital lobe (dashed circled area in the upper panel) was cut and flattened (lower panel). **b**. Axial sections of monkey 1's (upper panel) and monkey 2's (lower panel)

occipital lobes at the position indicated by the green dashed line in panel a. The outward borders of white and gray matter are highlighted by green and orange dotted lines, respectively. The lesions are evident by the absence of gray matter (red line markers). **c.** To compare visually elicited responses in extrastriate cortex in the presence versus absence of V1 input, rotating checkerboard stimuli were spatially restricted (2° diameter) and presented either inside (upper panel) or outside (lower panel) the scotoma (part of the visual field affected by the V1 lesion, indicated here by red circles).

Author Manuscript

Author Manuscript

Author Manuscript

Author Manuscript

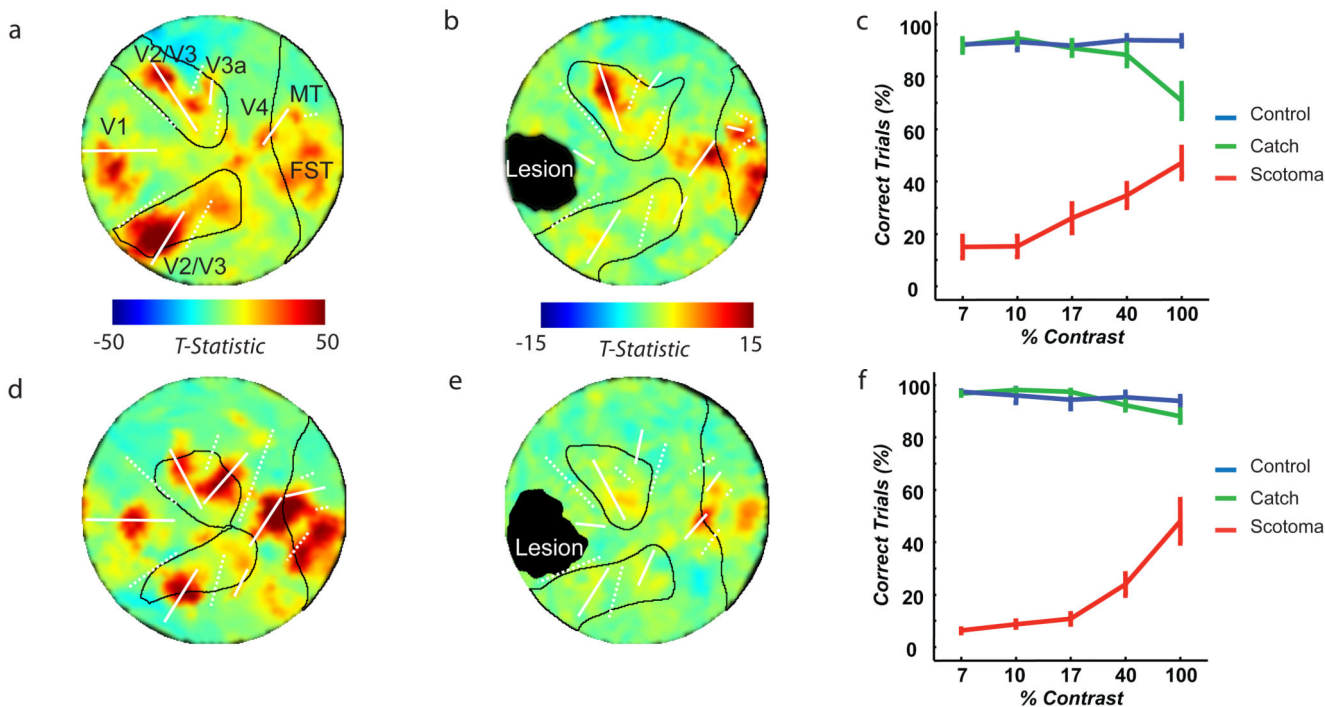


Figure 2.

Visual processing in V1 lesioned monkeys. **a.** Functional activation map of macaque 1's non-lesioned visual cortex to 85 cycles of visual stimulation outside the scotoma (figure 1C, lower panel). The map has been horizontally flipped for easier comparison with the lesioned hemisphere. White dotted and solid lines show the position of the vertical and horizontal meridian representations, respectively, derived from independent retinotopic mapping experiments (supplementary figures 1, 2) to reveal the functional boundaries of extrastriate areas6. **b.** Activation map of macaque 1's lesioned hemisphere to 85 visual stimulation cycles inside the scotoma (figure 1C, upper part). The position of the stimulus inside the scotoma was effective, in that lesion surrounding V1 cortex with intact gray matter was not activated. In the absence of V1 input, areas V2/V3, V4 and V5/MT continue to be visually responsive. **c.** Behavioral performance of monkey 1 in detecting visual stimuli (0.2° diameter) presented inside (red line) or outside (green line) the scotoma at different luminance contrast levels compared to a constant gray background. On one third of the trials no stimulus was presented and the monkey was rewarded for maintaining central fixation (blue line). Data represent mean \pm sem from five experiments. **d.** Functional activation map of monkey 2's non-lesioned hemisphere to 95 visual stimulation cycles. **e.** Activation map of monkey 2's lesioned hemisphere to 95 visual stimulation cycles inside the scotoma. **f.** Behavioral performance of monkey 2 for detecting visual stimuli inside (red line) versus outside (green line) the scotoma or during catch trials (blue line). Data represent mean \pm sem from five experiments. Although both monkeys display a large visual deficit, visual information continues to be processed to some extent as performance improves with stimulus contrast.

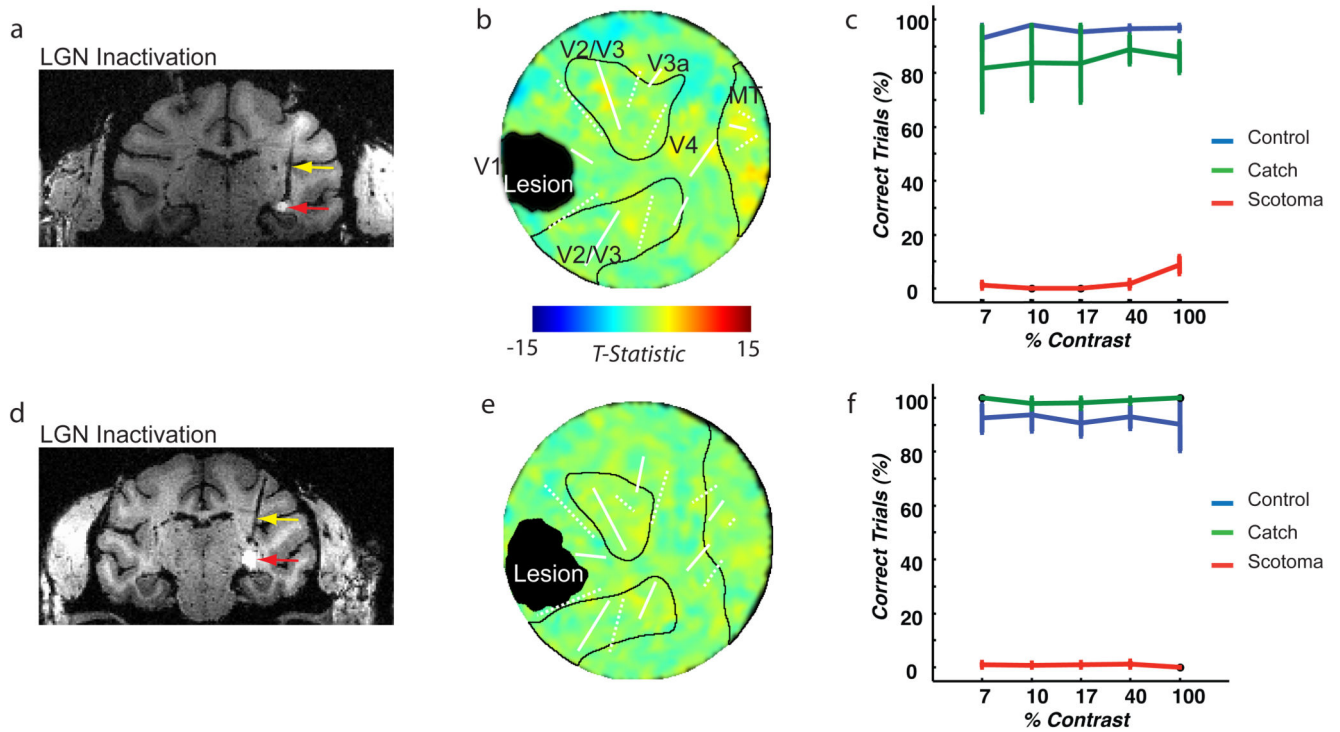


Figure 3.

Role of the LGN in driving V1-independent visual processing. **a.** Inactivation of the LGN was achieved by injecting the GABA-A agonist THIP (methods). The drug was co-injected (total volume 2 μ l, methods) with the diamagnetic MR contrast agent Gadolinium (Gd) to visualize the injection in MR images. Here, a coronal section through the posterior part of monkey 1's LGN (\sim AP +7 mm) is shown. Injection of Gd resulted in a localized increase in the intensity of the MR signal with a diameter of \sim 3 mm (red arrow). Reproducible injections across experiments were achieved by permanently implanting a MR-compatible cannula (yellow arrow). **b.** Functional activation map of macaque 1's left, lesioned hemisphere to visual stimulation inside the scotoma (35 stimulation cycles) during inactivation of the LGN. LGN inactivation results in the elimination of V1-independent visual responses (figure 2 b). **c.** Monkey 1's performance in detecting visual targets at different luminance contrasts. Data represent mean \pm sem performance from three experiments with THIP injections into the LGN. The injections eliminated the monkey's ability to detect a target inside the scotoma. **d.** Inactivation of macaque 2's posterior LGN. **e.** Activation map of macaque 2's right, lesioned hemisphere to visual stimulation inside the scotoma (60 stimulation cycles) during LGN inactivation. **f.** Monkey 2's performance for correctly detecting targets during LGN inactivation. Data represent the mean \pm sem performance in three experiments with THIP injections.

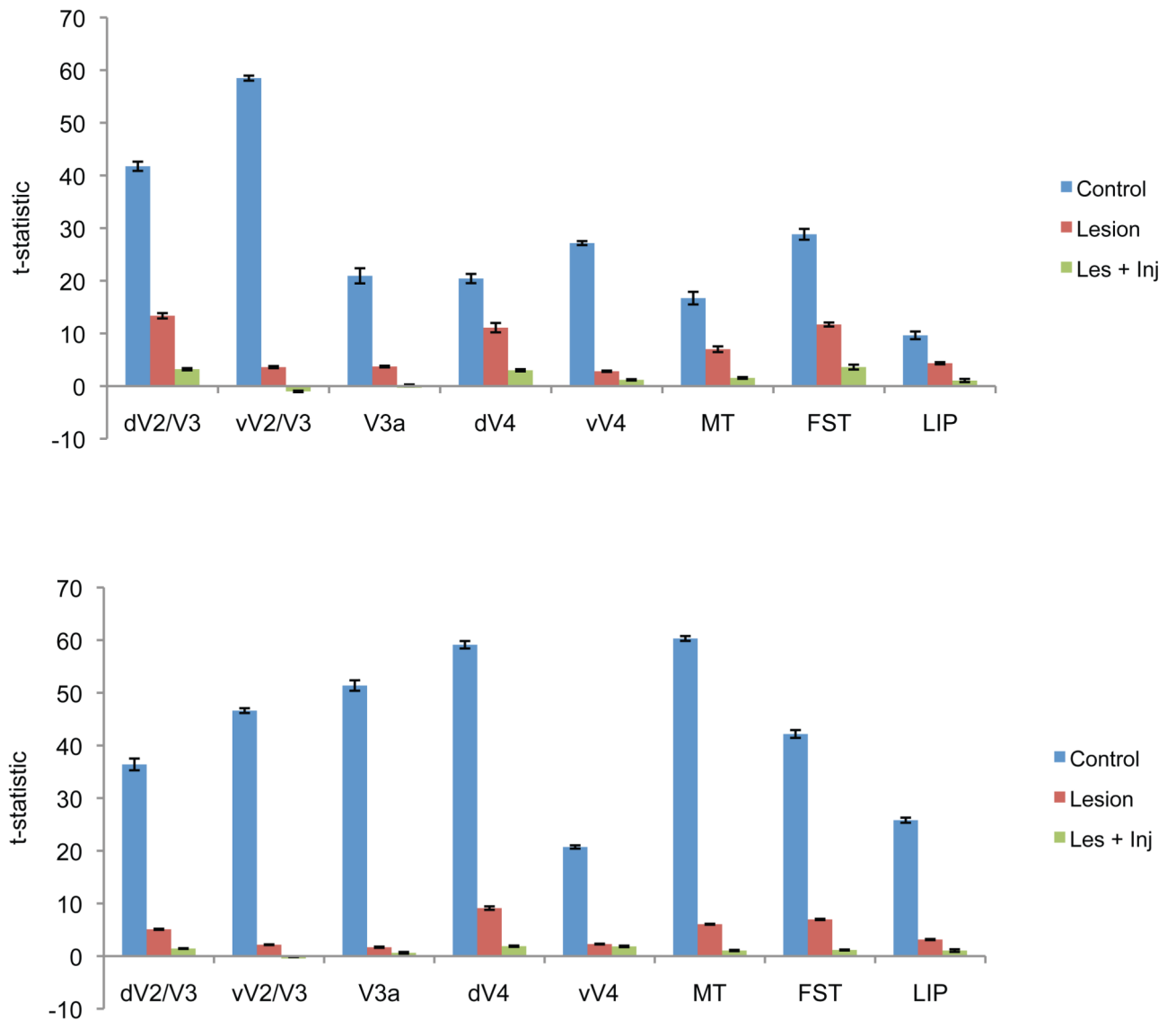


Figure 4.

Quantitative summary of mean fMRI activation levels in extrastriate areas under normal conditions (V1 and LGN intact, blue bars), in the absence of V1 input (lesion, red bars), and in the absence of input from V1 and the LGN (les. + inj., green bars). Data in the upper part were collected from monkey 1 and correspond to the mean \pm sem t-statistic obtained during 85 visual stimulation cycles without LGN inactivation and 60 stimulation cycles with LGN inactivation. Data in the lower part come from experiments with monkey 2, in which the mean \pm sem t-statistic has been computed over 95 stimulation cycles without LGN inactivation and 20 stimulation cycles with LGN inactivation. Note that on average across areas and monkeys, fMRI activation in extrastriate areas is reduced by ~80% when V1 input is missing. Additional LGN inactivation reduces activity by more than 95% compared to normal levels.